Three-dimensional optoacoustic mesoscopy of the tumor heterogeneity *in vivo* using high depth-to-resolution multispectral optoacoustic tomography

Jiao Li [a], Songhe Zhang [a], Andrei Chekkoury [b, c], Sarah Glasl [b, c],Paul Vetschera [b, c], Benno Koberstein-Schwarz [b, c], Murad Omar [b, c], and Vasilis Ntziachristos [b, c, *]

[a]School of Precision Instruments and Optoelectronics Engineering, Tianjin University, Weijin Str. 92, 300072 Tianjin, China; [b]Institute for Biological and Medical Imaging, Helmholtz Zentrum München, Deutsches Forschungszentrum für Gesundheit und Umwelt (GmbH), IngolstädterLandstr.,85764 Neuherberg, Germany; [c]Chair for Biological Imaging, Technische Universität München (TUM), Ismaningerstr. 22, 81675 München, Germany;

ABSTRACT

Multispectral optoacoustic mesoscopy (MSOM) has been recently introduced for cancer imaging, it has the potential for high resolution imaging of cancer development *in vivo*, at depths beyond the diffusion limit. Based on spectral features, optoacoustic imaging is capable of visualizing angiogenesis and imaging cancer heterogeneity of malignant tumors through endogenous hemoglobin. However, high-resolution structural and functional imaging of whole tumor mass is limited by modest penetration and image quality, due to the insufficient capability of ultrasound detectors and the two-dimensional scan geometry. In this study, we introduce a novel multi-spectral optoacoustic mesoscopy (MSOM) for imaging subcutaneous or orthotopic tumors implanted in lab mice, with the high-frequency ultrasound linear array and a conical scanning geometry. Detailed volumetric images of vasculature and oxygen saturation of tissue in the entire tumors are obtained *in vivo*, at depths up to 10 mm with the desirable spatial resolutions approaching 70μm. This unprecedented performance enables the visualization of vasculature morphology and hypoxia conditions has been verified with *ex vivo* studies. These findings demonstrate the potential of MSOM for preclinical oncological studies in deep solid tumors to facilitate the characterization of tumor's angiogenesis and the evaluation of treatment strategies.

Keywords: *In vivo* tumor imaging, optoacoustic mesoscopy, multi-spectral, angiogenesis, hypoxemia

1. INTRODUCTION

The application of optical imaging to *in vivo* preclinical studies of tumor angiogenesis, tumor hypoxia and tumor dynamics is important in revealing complex biological underpinning cancer, elucidating the tumor microenvironment, and leading to new treatment strategies [1-8]. Current pure optical imaging techniques for tumor visualization, however, only provide high-resolution images superficially or degrading spatial and quantificational information at the depth over few hundred microns caused by the strong optical scattering of biological tissues [1-5]. Optoacoustic imaging (also referred to as photoacoustic or thermoacoustic imaging) is inherently suited to offer high optical contrast and spectral specificity images with the microscale resolution beyond the penetration limits of ballistic optical methods, through combining advantages of optical and ultrasonic methods [2, 3, 9].

Optoacoustic mesoscopy enable imaging deeper than a few millimetres (1-10mm) with spatial resolution less than 100μm [10, 11]. With spectral specificity contrast and spectral unmixing techniques, multispectral optoacoustic mesoscopy has shown great potential in revealing the heterogeneity of entire solid tumors with high spatial resolution not captured by microscopy and macroscopy. *In vivo* Optoacoustic mesoscopic (OAM) imaging has been applied to subcutaneous or orthotopic tumors implanted in lab mice for the preclinical cancer research [12-15]. However, OAM approaches employing single element detectors in a planar detection geometry for three-dimensional (3D) imaging limit tomographic data

* v.natziachristos@tum.de

Photons Plus Ultrasound: Imaging and Sensing 2017, edited by Alexander A. Oraevsky, Lihong V. Wang, Proc. of SPIE Vol. 10064, 100643C · © 2017 SPIE · CCC code: 1605-7422/17/$18 · doi: 10.1117/12.2253047

collection to 2D scans, degrading image performances in the isotropic in-plane resolution, visibility of directional objects and temporal resolution in volumetric measurements at multi-wavelength excitation [12, 13].

A novel multi-spectral optoacoustic mesoscopy (MSOM) with linear arrays and translate-rotate scanning mode has been investigated in our group [10, 11, 14].To break through the limits of state-of-art methods for *in vivo* imaging tumor heterogeneity, we develop an innovative arrangement to enhance image performances by implementing MSOM at 15MHz central frequency with a conical scanning geometry. These implementations lead to high sensitive measurements, for example the 15MHz ultrasound linear array with higher sensitivity and more suitable frequency band for different sized vascular structures or absorbers in the tumor mass [14]. We apply these techniques to the tumor model of 4T1 *in vivo* and obtain detailed volumetric images of vasculature and oxygen saturation of tissue at depths up to 10 mm with sub-100-μm spatial resolution. Finally we show that these unprecedented performances in resolving the tumor vasculature morphology and hypoxemia conditions have been verified with the *ex vivo* study.

2. METHODS

2.1 Experimental setup and data acquisition

As shown in Fig. 1(A), the MSOM system built in our group has been redesigned with a conical scanning geometry to accommodate *in vivo* imaging of tumors [10]. The translate-rotation scanner can be implemented in two different scanning procedures, described in the detail in Ref. 14, with one rotation-motorized stage and one translation-motorized stage (M-062.PD and M-605.2DD, Physik Intrumente GmbH, Germany). We scan *in vivo* samples in the continuous acquisition mode with a rotation range of 255º and a translation range of 10 mm. Optical excitation is generated from a tunable (690 to 900 nm) optical parametric oscillator laser (Phocus II, Opotek Inc., Carlsbad, California), providing sub-10 ns pulses with a 10 Hz repetition rate and a maximum energy of 80mJ/pulse (760nm). The laser beam is delivered to imaging samples via a custom-made 640-fiber bundles in four arms. To accommodate *in vivo* imaging of tumors, four fiber arms are fixed on one side as shown in Fig. 1(B).

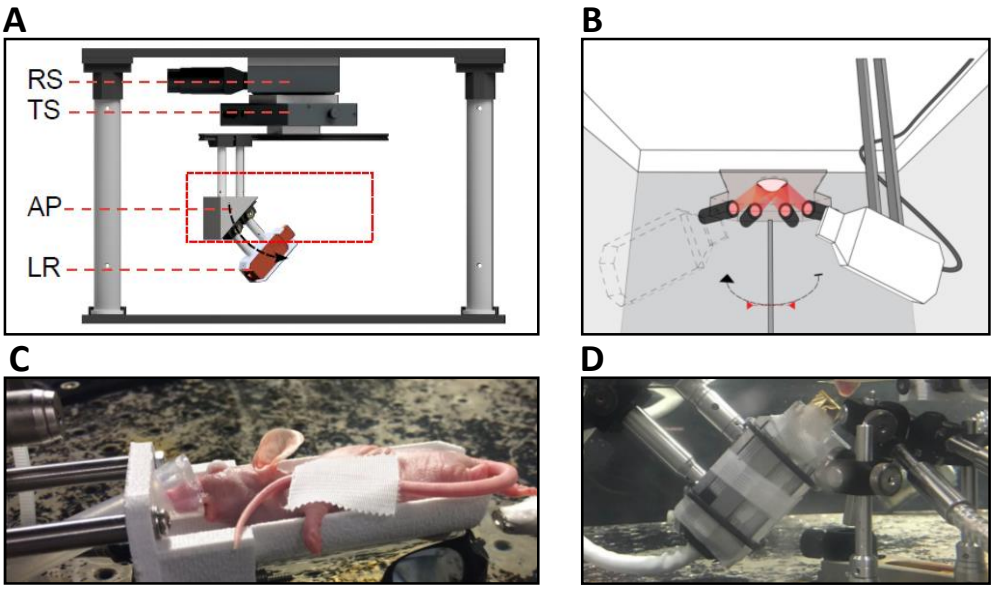

Figure 1. The experimental setup of MSOM for *in vivo* small-animal tumor imaging:(A) Schematic of the experimental setup: A linear array (LR) with 45-degree titling angle, connected to a translation-rotation scanning system combing a translation stage (TS) and a rotation stage (RS), providing three-dimensional volumetric measurements; The LR and tumor in mouse are covered in water for the acoustic coupling. The details of the adapting plate (AP) is shown in (B). (B) Schematic of the implantation sites of tumor in a mouse with four-arm fiber bundles. Arrows with black dash lines and read dash lines indicate the rotation and translation trajectory of linear array, respectively. (C) The photograph of experimental mouse with the anesthesia mask on the mouse holder. (D) The photography of the tumor, the linear array and fiber bundles under the water.

Ultrasound detection is based on a custom-made linear array with 96 elements, a 15 MHz central frequency and an average -6 dB pulse-echo bandwidth of 45%. As shown in Fig.1 (A), the array is mounted on 45-degree titling module

used to provide a conical scanning geometry for *in vivo* imaging of tumors. The linear array is continuously rotated and translated at the predefined speeds based on the repetition rate of the laser, with the rotation angle of ~0.035º and the translation distance of ~200 nm between two successive laser pulses. The signal-pulse acquisitions (~7000) at one wavelength are digitized a custom-built data acquisition card at 125 MS/s and 12 bit resolution over a 16 mV range, with the total scanning time of 12 mins. Image procedures are performed under general anesthesia (1.8% isoflurane with 100% O_2), as shown in Fig. 1(C). The heads of fiber bundles, the linear array and tumors/samples are immersed in a water tank with a stable temperature of 33 ºC for acoustic coupling (Fig. 1(D)).

2.2 Phantom and animal preparations

To characterize the MSOM system, phantom 1 consisting of 20 μm diameter black microspheres, which are randomly dispersed in agar gel, is molded to form cylinders of 12 mm diameter. The broadband optoacoustic signals generated by this absorbers have higher frequency than the maximum of the linear array considering the duration of the laser pulses. Therefore, phantom 1 could be used to calibration the MSOM, determine an average speed of sound and assess the spatial resolutions of the system. Procedures involving animals measured under general anesthesia were approved by the government of Upper Bavaria. The cancer cell line of 4T1 mouse mammary tumor cells (CRL-2539) was used. The 5-week-old mice (female athymic Foxn1 nude mice) were inoculated with the cell suspensions (4T1: 100 thousand cells) into the mammary pad. The experiment is implemented when tumors reached ~8 mm diameter (4T1: day 8).

2.3 Image reconstruction methods

Raw acquired data are bandpass filtered using the 3rd Butterworth filter between 1 MHz and 30 MHz for noise removal. The filtered data are then treated with a time-variant filter to compensate the acoustic attenuation depending on the acoustic frequency [16]. The 3D images are reconstructed using a filtered backprojection formula [17] with the voxel size of 24μm × 24μm × 24μm. After image reconstructions of all the selected wavelengths and light fluence correction, a linear spectral unmixing algorithm is applied to obtain the functional images representing distribution of endogenous contrast agents Functional images are colored, composited and analyzed using Amira without any image processing.

3. RESULTS

Figure 2 demonstrates the optoacoustic results performed from phantom 1, used to characterize the image performance of the proposed MSOM system for 3D visualization capabilities. The profiles along different axes have been shown beside the magnification images of a 20 μm microsphere. The calculated full width at half maximum (FWHM) of those profiles are 74.4 μm and 74.2μm, respectively.

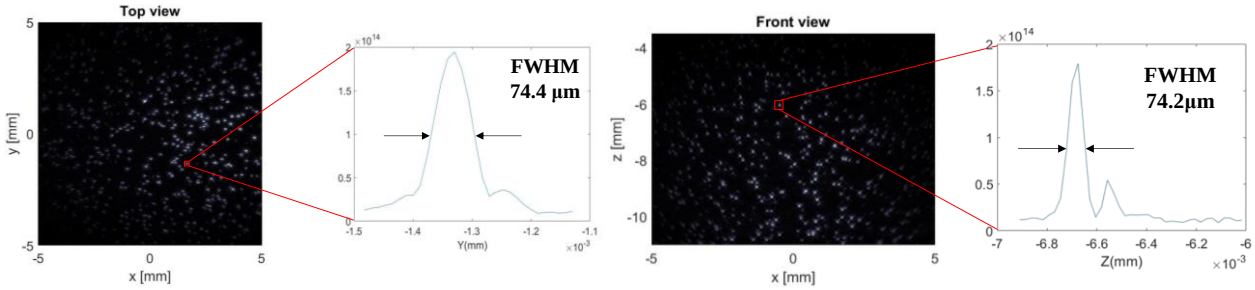

Figure 2. Reconstruction images of phantom 1 (20μm microspheres): maximum intensity projection (MIP) images along the Z-axis (Top view) and Y-axis (Front view); Red squares show a selected microsphere with the normalized profiles. The FWHM of the profiles along Y-axis and Z-axis are 74.4μm and 74.2μm, respectively.

Figure 3 demonstrates label-free results from the *in vivo* tumor (4T1) imaging, performed to validate the functional image performance of the proposed MSOM in living system. An orthotopic tumor was measured on 8th day from injecting the 4T1 tumor cells (100 thousands) into the mammary pad. Fig. 3(A) shows the photograph of experimental tumor. 3D view and side view of the OAM image of the entire solid tumor at 750nm have been shown in Fig. 3(B) and (C), containing complicated multi-scale vascular network, representing the tumor angiogenesis and surrounding feeding vessels. Fig. 3(D) and (E) demonstrate the functional hemoglobin (HbO_2 and Hb) images of the 4T1 tumor. It is observed that feeding vessels on the surface of the tumor and close to the mouse body are HbO_2-dominated, but the internal tumor vasculature renders the lump feature with high concentrated distribution of Hb. The scattered massive distribution inside the tumor can also be obviously visualized in the Fig.2 (C).

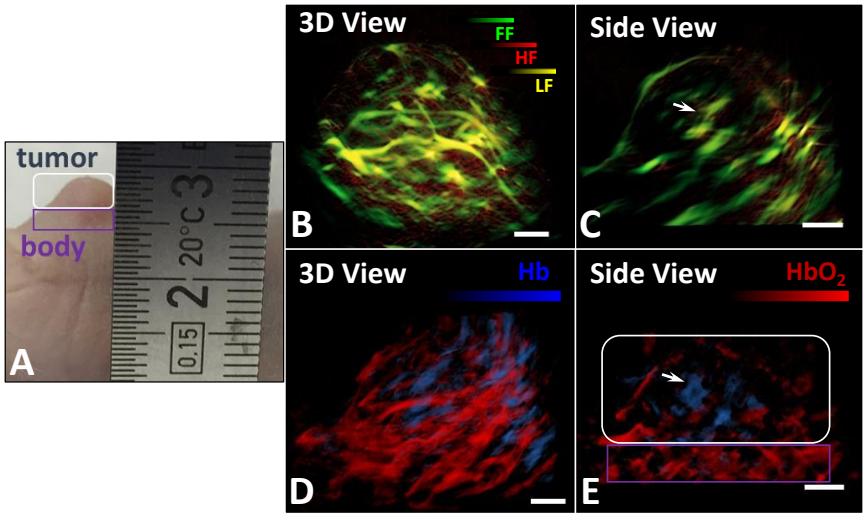

Figure 3. Label-free functional imaging *in vivo* of the orthotopic 4T1 tumor using MSOM. (A) The photograph of experimental tumor with tumor mass (the white square) and the part of mouse body (the purple square) in the measured region. (B) and (C) are the 3D view and side view of the OAM image at 750nm colored by frequency content of different structures in tumor: Full frequency (FF); High frequency (HF); Low frequency (LF); (D) and (E) are the 3D view and side view of the functional hemoglobin (HbO_2 and Hb) image of a 4T1 tumor (day 8), with the squares corresponding to the ones in (A). The white arrow indicates the tumor core in (C) and (E).

Figure 4 illustrates the comparison between functional optoacoustic results and classic cryosection images, for validating accuracy and fidelity of reconstructed images by the proposed MSOM. After the MSOM measurement, the mouse with an orthotopic 4T1 tumor was sacrificed and prepared for frozen section analysis. Fig. 4(A-C) depict the 3D view, front view and side view of MSOM results and corresponding cryosection images, respectively. It is clearly observed that higher OAM regions have close correspondence to the areas close to feeding vessels or the core of tumor in the cryosection images. Fig. 4(D-F) demonstrate maximum intensity projection (MIP) images along the Z-axis (Top view) of the selected regions 1-3 in Fig. 4(C), respectively, which also present the highlighted areas in MSOM results correlating well to the cryosection images.

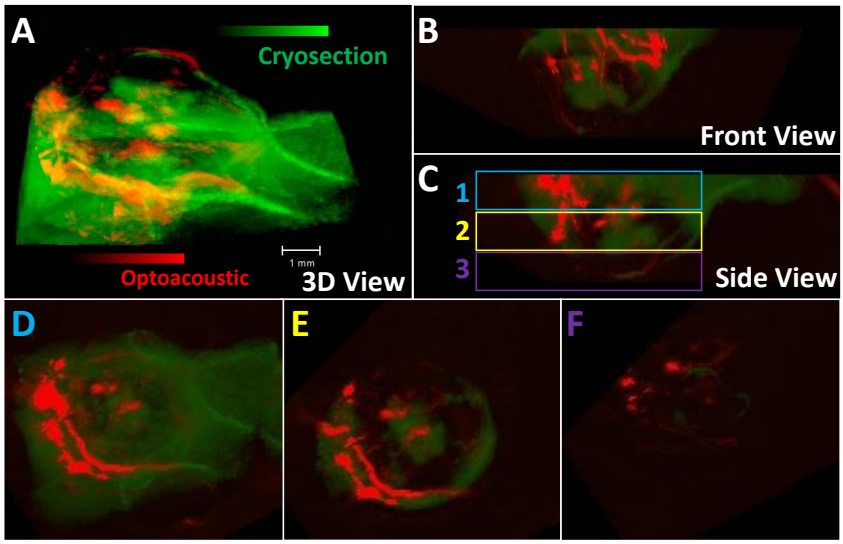

Figure 4. Comparison of OAM and cryosection images. (A) 3D view, (B) front view and (C) side view of OAM and cryosection images of the 4T1 tumor, where the 3D cryosection image is extracted from the cryosection photographs of the entire tumor. (D), (E) and (F) are X-Y MIPs of three regions indicated in (C).

4. DISCUSSION AND CONCLUSION

This study has shown that it is possible, with use of MSOM, to provide high-fidelity 3D *in vivo* images of endogenous contrast including hemoglobin and oxygenation, with sub-100-μm spatial resolution at depths up to 10 mm seeing through the tumor mass. The increased quality of functional images can be achieved by the proposed MSOM, compared with OAM systems based on planar detection geometry [14]. Because the linear array with the center frequency of 15MHz is available to attain high-SNR multi-wavelength volumetric measurements detected from both sub-100-μm absorbers and up to several millimeter necrotic core. Furthermore, MSOM can achieve higher temporal resolution at multi-wavelength excitation and real volumetric measurements for 3D tomography mode, yielding high-fidelity functional images of the whole tumor bulk. The potential application of the proposed MSOM as a tool for imaging tumor heterogeneity has been demonstrated by acquiring 3D high-fidelity hemoglobin-functional images of the entire 4T1 tumor, really seeing deep into the tumor core. This indicates that tumor-related vascularization features, such as vasculature patterns, oxygenation and necrosis, could be observed *in vivo* and strictly non-invasively (i.e. label-freely).The study shows the potential of MSOM for studying the organization of both tumor angiogenesis and tumor microenvironment (i.e. hypoxia), and evaluating existing therapeutic approaches, such as antiangiogenic therapy, vascular normalization as a therapeutic strategy and hypoxia-targeting therapy [6-8].

In summary, MSOM could be considered as a promising imaging instrument in preclinical cancer researches for studying tumor angiogenesis and hypoxia. The proposed MSOM should be possible used to follow the development of tumors over time with or without therapeutic interventions. Performing studies on monitoring treatment processes or observing other biological applications will be main subjects of further investigations.

ACKNOWLEDGEMENTS

The authors acknowledge the funding supports from the National Natural Science Foundation of China (81401453), and the scholarship from China Scholarship Council (CSC) under the Grant CSC NO. 201506255001.

REFERENCES

[1] Vasilis Ntziachristos, "Going deeper than microscopy: the optical imaging frontier inbiology," Nature Methods 7(8), 603-614 (2010).
[2] Adrian Taruttis, Gooitzen M. van Dam, and Vasilis Ntziachristos, "Mesoscopic and macroscopic optoacoustic imaging of cancer," Cancer Research 75(8), 1548-1559 (2015).
[3] Srivalleesha Mallidi, Geoffrey P. Luke, and Stanislav Emelianov, "Photoacoustic imaging in cancer detection, diagnosis, and treatment guidance," Trends Biotechnol 29(5), 213-221 (2011).
[4] Judith Weber, Paul C Beard and Sarah E Bohndiek, "Contrast agents for molecular photoacoustic imaging," Nature Methods 13(8), 639-650 (2016).
[5] Lihong V Wang and Junjie Yao, "A practical guide to photoacoustic tomography in the life sciences," Nature Methods. 13(8), 627-638 (2016).
[6] Peter Carmeliet and Rakesh K. Jain, "Principles and mechanisms of vessel normalization for cancer and other angiogenic diseases," Nature Reviews 10(6), 417-427 (2011).
[7] Annamaria Rapisarda and Giovanni Melillo, "Overcoming disappointing results with antiangiogenic therapy by targeting hypoxia," Nature Reviews 9(7), 378-390 (2012).
[8] Sara M Weis & David A Cheresh, "Tumor angiogenesis: molecular pathways and therapeutic targets," Nature Medicine 17(11), 1359-1370 (2011).
[9] Jérôme Gateau, Andrei Chekkoury and Vasilis Ntziachristos, "Ultra-wide band three-dimensional optoacoustic tomography," Optics Letters 38(22), 4671-4674 (2013).
[10] Jérôme Gateau, Andrei Chekkoury and Vasilis Ntziachristos, "High-resolution optoacoustic mesoscopy with a 24 MHz multidetector translate- rotate scanner," Journal of Biomedical Optics 18(10), 106005 (2013).
[11] Andrei Chekkoury, Jérôme Gateau, Wouter Driessen, Panagiotis Symvoulidis, Nicolas Bézière, Annette Feuchtinger, Axel Walch and Vasilis Ntziachristos, "Optical mesoscopy without the scatter: broadband multispectral optoacoustic mesoscopy," Biomedical Optics Express 6(9), 3134-3148 (2015).

[12] Jan Laufer, Peter Johnson, Edward Zhang, Bradley Treeby, Ben Cox, Barbara Pedley, and Paul Beard, "In vivo preclinical photoacoustic imaging of tumor vasculature development and therapy," Journal of Biomedical Optics 17(5), 0560161-0560168 (2012).
[13] Murad Omar, Mathias Schwarz, Dominik Soliman, Panagiotis Symvoulidis and Vasilis Ntziachristos, "Pushing the Optical Imaging Limits of Cancer with Multi-Frequency-Band Raster-Scan Optoacoustic Mesoscopy (RSOM)," Neoplasia 17(2), 208-214 (2015).
[14] Andrei Chekkoury, Antonio Nunes, Jerome Gateau, Panagiotis Symvoulidis, Annette Feuchtinger, Nicolas Beziere, Saak V. Ovse pian, Axel Walch and Vasilis Ntziachristos, "High-Resolution Multispectral Optoacoustic Tomography of the Vascularization and Constitutive Hypoxemia of Cancerous Tumors," Neoplasia 18(8), 459-467 (2016).
[15] Amit P. Jathoul, Jan Laufer, Olumide Ogunlade, Bradley Treeby, Ben Cox, Edward Zhang, Peter Johnson, Arnold R. Pizzey, Brian Philip, Teresa Marafioti, Mark F. Lythgoe, R. Barbara Pedley, Martin A. Pule and Paul Beard, "Deep in vivo photoacoustic imaging of mammalian tissues using a tyrosinase-based genetic reporter," Nature Photonics 9(4), 239-246 (2015).
[16] Bradley E. Treeby, "Acoustic attenuation compensation in photoacoustic tomography using time-variant filtering," Journal of Biomedical Optics 18(3), 036008 (2013).
[17] Jérôme Gateau, Miguel Ángel Araque Caballero, Alexander Dima and Vasilis Ntziachristos, " Three-dimensional optoacoustic tomography using a conventional ultrasound linear detector array: Whole-body tomographic system for small animals," Med. Phys 40(1), 013302 (2013).